THE TRIGGERED BEHAVIOUR OF A CONTROLLED CORONA STABILISED CASCADE SWITCH

M. J. Given [*], **M.P. Wilson, I.V. Timoshkin, S.J. MacGregor, T. Wang**
Dept. Electronic & Electrical Engineering, University of Strathclyde, 204 George Street, Glasgow, G1 1XW, UK

J.M. Lehr
Sandia National Laboratories, P.O. Box 5800, Albuquerque, NM 87185, USA

Abstract
Corona stabilised switches have been shown to have advantages in pulse power switching applications due to their high repetition rates and low jitter. Work performed in recent years by the High Voltage Technologies Group within the Department of Electronic and Electrical Engineering at the University of Strathclyde has shown that the operating voltage range of such switches can be extended by using a multi-gap cascade configuration. One particular multi-gap topology was shown to operate under pressure at 100 kV with a switching jitter of ≈ 2ns. It has since been shown that by modifying the topology of the corona sources on the electrodes, it is possible to control the grading of the voltage distribution across the gaps in the cascade. The voltages across each gap and the self-break behaviour of the cascade were found to be in close agreement with the values predicted from the corona emission characteristics for the tested electrode topologies. This paper reports on a further examination of the behaviour of the corona controlled switching topology, where triggered operation of the switch has been investigated for different voltage distributions across the cascade gaps.

I. INTRODUCTION

There is interest in developing cascade switches that operate in a corona stabalised mode. Such switches should have the advantages shown by single stage corona stabalised switches: low jitter and a high repetition rate [1,2], while being capable of switching significantly higher voltages in the range of 100kV. An advantage of corona stabalised cascades is that the voltage grading across the gaps in the cascade is resistive rather than capacitive, due to the presence of the plasma introduced by the corona discharges. This results in a voltage distribution across the cascade elements that is robust and unaffected by stray capacitances between the cascade elements and its surroundings. The operation of such a switch with a jitter of ~ 2ns has been reported by the authors.

In the original switch geometry described in [3] the corona generating elements on each of the electrodes in the cascade were identical, consisting of an edged cylinder protruding 15mm from the electrode with an internal diameter of 30mm. The gap spacing between each of the cascade elements was also identical. This approach should lead to a uniform division of the switching voltage across the gaps of the cascade.

In later work the possibility of controlling the corona emission characteristics of the individual electrodes in the cascade was explored [4]. This was achieved by altering the diameter of the corona emitting electrodes. It was shown that it was possible to control the voltage distribution across the cascade elements in a predictable manner by varying the corona electrode geometries and to accurately predict the hold-off voltage for the corona controlled cascade. This paper describes some initial results on the triggered behaviour of such a cascade.

II. BASIS OF CORONA CONTROL OF CASCADE VOLTAGES

In [4] the authors assumed that the behaviour of corona current in a gap of the cascade took a form similar to that defined by Sigsmond [5] for the corona current in a point plane geometry:

$$I(V) = I_0 \left(V - V_0\right)^2 \qquad (1)$$

where V_0 is the corona initiation voltage. The parameter I_0 was a modification of that defined by Sigsmond assuming that the corona current would be proportional to the circumference of the edge of the corona generating electrode:

$$I_0 = \frac{r}{d}\alpha, \quad \alpha = 4\pi k\mu\varepsilon \qquad (2)$$

where r is the radius of the corona generating electrode, d is the separation between electrodes, μ is the effective

[*] e-mail: m.given@eee.strath.ac.uk

mobility for the charge carriers, ε is the permittivity of the region where the corona discharge is occurring, and k is a constant defining the number of corona sources per unit length of the electrode.

The behaviour of the corona current as the radius r and gap spacing d were varied has been measured and shown to follow the behaviour predicted in (1). This allowed the parameters I_0 and V_0 to be determined for different radii and gap spacings . The behaviour of I_0 has also been shown to follow the behaviour of (2) [4].

In a n gap corona controlled cascade at equilibrium, current continuity requires that the currents in each individual gap, $I_1 ... I_n$ to be identical. Equation (1) can be rearranged to relate the voltage across an individual gap V_i to the common corona current I_C:

$$V_i = \sqrt{\frac{I_C}{I_{0i}}} + V_{0i} \tag{3}$$

where I_{0i} and V_{0i} define the corona emission characteristics for gap i.

The total voltage across the cascade V_{Cas} can therefore be expressed in terms of I_C in the form of:

$$V_{Cas} = \sum_{i=1}^{n}\left[\sqrt{\frac{I_C}{I_{0i}}} + V_{0i}\right] \tag{4}$$

Equation (4) can be rearranged to allow the corona current in the cascade I_C to be calculated in terms of the total voltage across the cascade V_{Cas}:

$$I_C = \frac{V_{Cas} - \sum_{i=1}^{n} V_{0i}}{\sum_{i=1}^{n}\left[\left(\frac{1}{I_{0i}}\right)^{\frac{1}{2}}\right]} \tag{5}$$

Equations (5) and (3) allow the voltage across each individual gap in the cascade to be predicted and the validity of this approach has been demonstrated by the authors [4]. In addition equation 5 indicates the criterion at which corona controlled distribution of voltage will occur across the gaps:

$$V_{Cas} - \sum_{i=1}^{n} V_{0i} > 0 \tag{6}$$

III. EXPERIMENTAL SYSTEM

The cascade was operated in air at ambient conditions. It contained three gaps; two diameters of corona forming electrodes were used: 6.5 and 12.5 mm. Gap spacings within the cascade were varied between 10 and 16mm. To characterise the triggered behaviour of the corona controlled cascade the test system shown in figure 1 was set up.

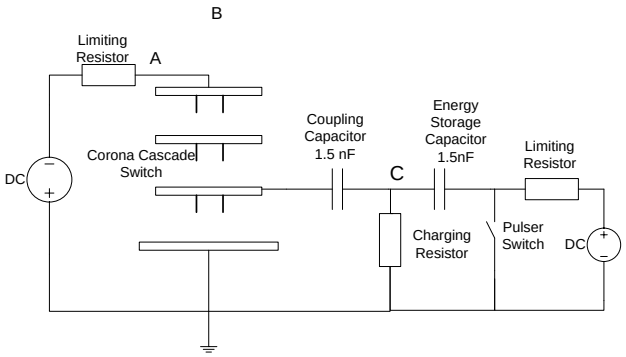

Figure 1. Diagram of experimental system: A Rogowski probe position; B location of D-dot probe; C location of voltage probe.

The system consisted of the cascade with the uppermost electrode connected to a negative d.c. power source (Glassman WR 100kV) through a 500kΩ limiting resistor. In operation the measured corona currents (0.5 to 1.5 mA) indicated that corona induced resistance of the gaps was of the order of (15 to 50 MΩ).

The lowest gap in the cascade was triggered using a simple inverting pulser. The pulser consisted of a 1.5nF capacitor rated at 80kV which was charged from a 0-60 kV d.c positive power source (Glassman EH) through a second 500kΩ limiting resistor. The switch to operate the pulser was of a simple mechanical design. The charging resistor for the pulser was a $CuSO_4$ resistor with a resistance measured as 4.2 kΩ. To prevent this resistor from appearing in parallel the with the corona induced resistance of the triggered gap of the cascade, a coupling capacitor of 1.5nF was used to connect the pulser to this gap.

When the corona controlled cascade was in operation it was not possible to monitor the voltages on the cascade or the triggering voltage directly, as the use of dividing voltage probes would have affected the voltage distribution across the gaps. Therefore the following instrumentation was used:

the current flowing in the cascade during the breakdown of the switch was monitored using a screened Rogowski coil placed round the connection between the limiting resistor and the top electrode of the cascade (A in Figure 1);

the voltage across the cascade was monitored using a D-dot probe. This consisted of a high frequency low voltage oscilloscope probe (Scopex) which was suspended 30 cm above the uppermost cascade electrode. (B in Figure 1);

the triggering voltage was monitored using a high voltage oscilloscope probe (Tektronix P6015A) which was connected to the point between the energy storage capacitor and the coupling capacitor (C in Figure 1).

The outputs of the three measurement probes were connected to a Tektronics TDS 3054C oscilloscope. Figure 2(a) shows a representative set of waveforms for the operation of the corona controlled cascade

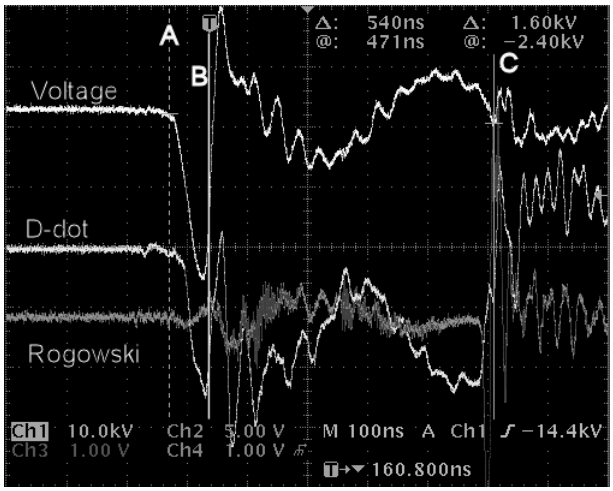

Figure 2(a). Output of diagnostics during triggered operation of cascade.

The upper trace in Figure 2(a) shows the output of the oscilloscope probe monitoring the pulser voltage used to trigger the cascade, the middle trace shows the output of the D-dot probe monitoring the voltage across the cascade while the lower trace shows the output of the Rogowski coil monitoring changes in current through the cascade. The following points are identified on the oscillogram:

(A) Start of switch operation, this is indicated by the appearance of a voltage signal from the probe monitoring the output of the pulser and a signal on the Rogowski probe output, figure 2(c) line A;

(B) Breakdown of triggered gap, this is indicated by a discontinuity in the signal observed in the output of the pulser and changes in the output of the D-dot probe figures 2(b) and 2(c) line B;

(C) Breakdown of full cascade, indicated by strong signals in both the Rogowski and D-dot probe outputs, figures 2(b) and 2(c) line C.

IV. WAVEFORM ANALYSIS

Integrating the output of the Rogowski probe should produce a signal proportional to the current flowing into the cascade from the d.c. source.

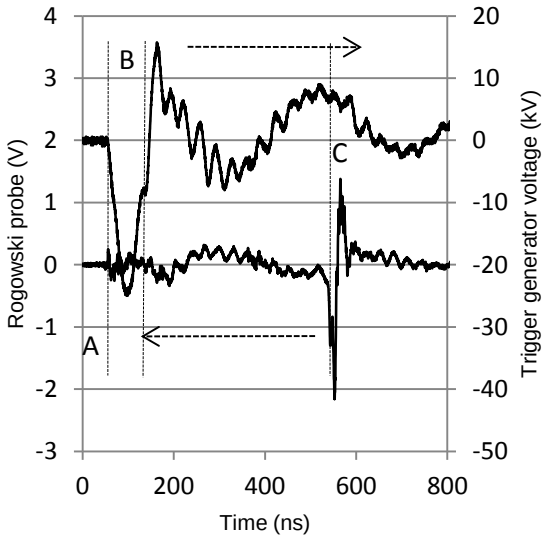

Figure 2(b). Output of pulser and Rogowski probe during cascade operation

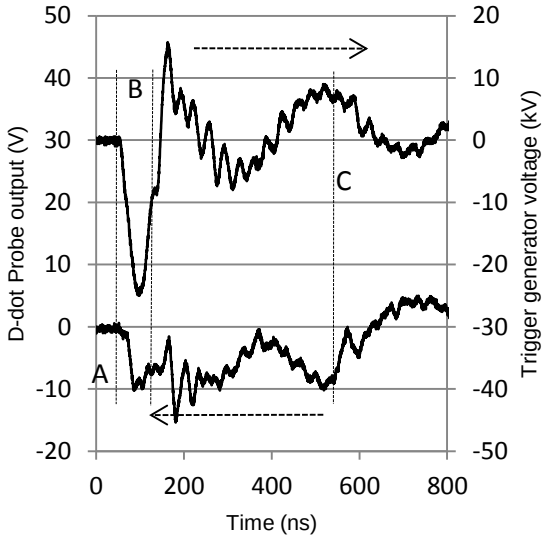

Figure 2(c). Output of pulser and D-dot probe during cascade operation

Figure 3(a) shows the integrated output of the Rogowski probe during cascade operation. As the probe is uncalibrated at present the absolute magnitude of the currents cannot be determined. A small peak in the current is observed during the application of the trigger pulse to the system, more clearly shown in figure 3(b). When the triggered gap breaks down a rapid increase in the current is observed, followed by a sinusoidal oscillation. This appears to be related to the oscillations observed by the voltage probe at the output of the pulser which show an under-damped sinusoidal response during this period. When the full cascade breaks down, a very

clear spike in the current is observed, superimposed on the sinusoidal oscillations.

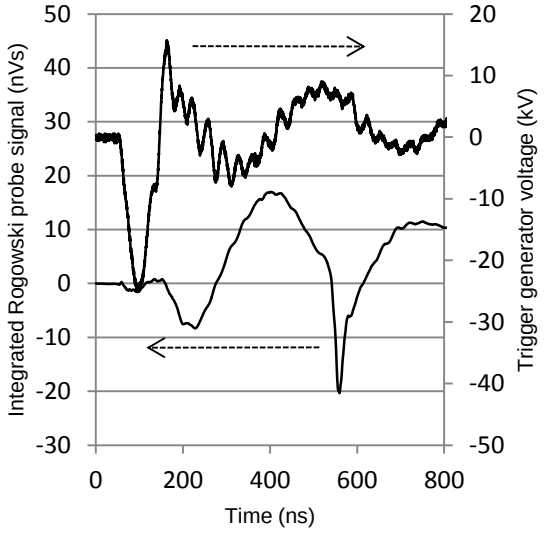

Figure 3(a). Integrated output of Rogowski probe during cascade operation

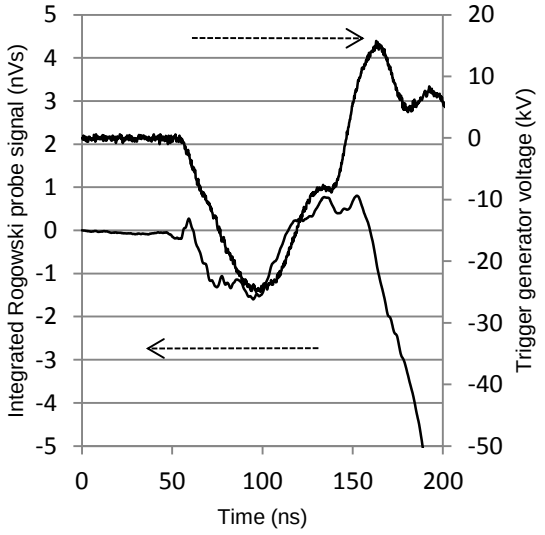

Figure 3(b). Integrated output of Rogowski probe during triggering of the cascade.

The behaviour of the current during triggering of the cascade is shown in figure 3(b). As the bottom gap of the cascade is driven to a more negative voltage a current is observed to flow into the cascade due to displacement. As the triggered gap breaks down, a clear transition in the behaviour of the current flowing in the cascade occurs.

Figure 4 shows the integrated output of the D-dot probe. This should be proportional to the electric field coupling to the probe and therefore to the voltage across the cascade. The D-dot probe is uncalibrated, for the results shown in Figure 4 the voltage across the cascade was 60 kV. The results suggest, that during the operation of the switch, the voltage across the cascade is falling at a generally uniform rate. There is some evidence of a finer structure in the integrated output, with changes of gradient occurring as the switch closes. These however appear to be correlated with the peaks observed in the oscillating voltage signal measured at the output of the pulser, so it is not possible to attribute these features to the breakdown of individual gaps within the cascade

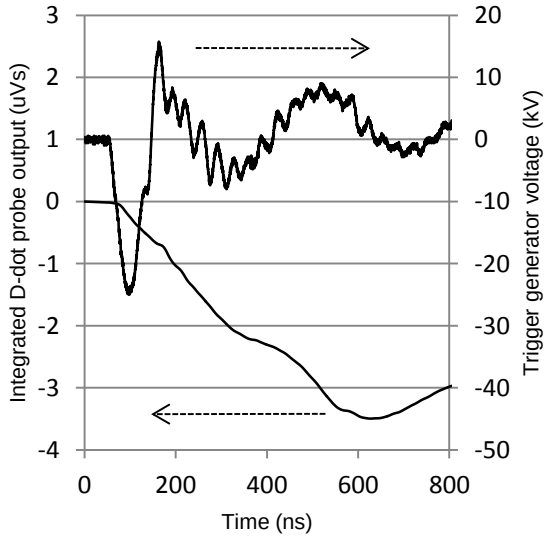

Figure 4. Integrated output of D-dot probe during cascade operation

V. TRIGGERED BREAKDOWN OF A SINGLE GAP.

To determine the expected triggered breakdown behaviour of the cascade it is first necessary to characterise the behaviour of triggered breakdown in individual corona stabilised gaps. The circuit in Figure 1 was used, with a single cascade element. The previous work with this electrode geometry had indicated that the d.c. self break voltage under ambient atmospheric conditions was of the order of 30 kV. It was assumed that the triggered electrode in the cascade would be operating at this voltage and that when the triggered gap was closed this voltage would be equally divided across the two remaining gaps.

Therefore the triggered behaviour of a single gap was investigated with the pulser charged to 15kV. Under these conditions the rise time of the pulser voltage to its maximum value occurred in ~ 50 ns. The peak voltage observed at the output of the pulser was 20kV due to the presence of inductance and ringing in the circuit. The d.c. corona voltage applied to the gap was varied up to 32 kV.

Figure 5(a) shows the time to breakdown behaviour of a 6.5 mm diameter corona forming electrode for gaps of 10, 12, 14 and 16 mm, as the d.c. voltage applied to the gap is varied. Figure 5(b) shows the triggered behaviour of a gap using a 12.5mm diameter corona electrode. These results are based on 30 measurements.

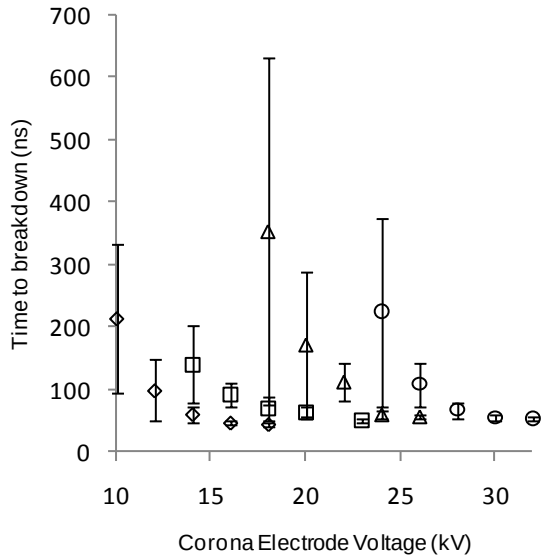

Figure 5(a). Triggered breakdown of single gap with 6.5mm corona forming electrode for four gap spacings: ◊ 10mm gap, □ 12mm gap, Δ 14 mm gap,○ 16 mm gap

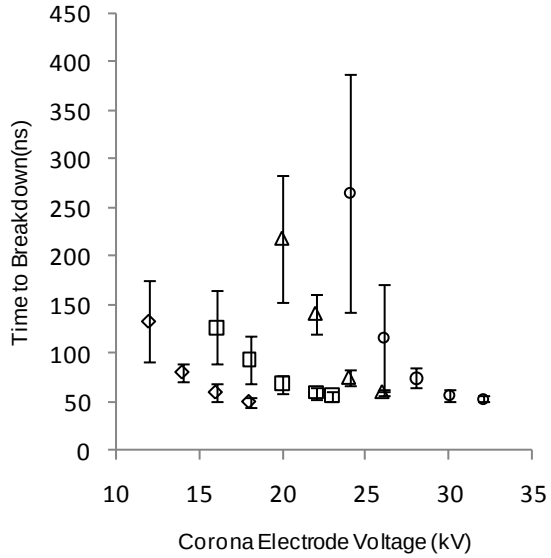

Figure 5(b). Triggered breakdown of single gap with 12.5 mm corona forming electrode for four gap spacings: ◊ 10mm gap, □ 12mm gap, Δ 14 mm gap,○ 16 mm gap

In both figures it can be seen that the time to breakdown and the jitter decreases as the d.c. voltage is increased. The average breakdown time seems to be longer for the 12.5 mm diameter electrode; however it is not possible to separate the measured behaviour of the two electrodes with confidence.

VI. TESTS ON 3 GAP CASCADE

A three gap cascade was set up and its breakdown behaviour was examined for two different configurations. In each configuration the lowest, triggered electrode used a 6.5mm diameter corona forming element, the two upper gaps used 12.5mm diameter corona forming elements. The first configuration (Cascade I) had the triggered gap set to 14mm and the remaining gaps in the cascade set to 12mm. The second configuration (Cascade II) set the triggered gap separation to 16 mm while the remaining gaps were kept at 12mm separation. Cascade I was tested at 60 kV and Cascade II was tested at 60 and 70 kV

Table 1 shows the predicted voltage distribution across the cascade gaps based on equations (5) and (3) and the data on the corona emission characteristics reported in [4]. The table also contains data on estimated jitter for gap closure based on the results reported in section V above on the operation of single gaps in triggered mode.

Table 1. Predicted Characteristics of Cascade

		Gap1	Gap 2	Gap 3
Cascade I 60 kV	Separation (mm)	14	12	12
	Voltage (kV)	22.2	18.9	18.9
	Jitter (ns)	31	>30	>30
Cascade II 60 kV	Separation (mm)	16	12	12
	Voltage (kV)	23.4	18.3	18.3
	Jitter (ns)	16	>40	>40
Cascade II 70 kV	Separation (mm)	16	12	12
	Voltage (kV)	28	21	21
	Jitter (ns)	5.2	7.8	7.8

As can be seen the predicted values for the jitter in Cascade I indicate that a poor performance is likely in this configuration. Cascade II at 60 kV has increased the voltage appearing across the triggered gap which should reduce the jitter in its closing. However the voltage across the untriggered gaps has been reduced which is likely to lead to an increase in the jitter for the untriggered sections of the cascade closing. When the voltage across Cascade II is increased to 70 kV, the voltage distribution is such that the predicted jitter for all the gaps in the cascade falls below 8ns.

Table 2. Measured Performance of the Cascade

		Triggered Gap	Rest of Cascade	Total Operation
Cascade I 60 kV	Time to breakdown (ns)	72.1	436	508
	Jitter (ns)	29.9	90.5	93.3
Cascade II 60 kV	Time to breakdown (ns)	57	391	448
	Jitter (ns)	9.96	81.2	88.2
Cascade II 70 kV	Time to breakdown (ns)	56.6	148	204
	Jitter (ns)	6.31	12.4	12.8

Table 2 shows the measured performances for the two cascade configurations. 30 measurements were taken in each case. The time to breakdown measurements for the triggered gap was the interval between the points A and B shown in figure 1. The time to breakdown for the rest of the cascade was the interval between points B and C. The closing time for the complete switch was the interval between points A and C

It can be seen that as expected from the data in Table 1 the performance of Cascade I with an operating voltage of 60 kV is poor with a jitter in the total run time of the switch of the order of 90ns. The jitter in the closing of the triggered gap is in good agreement with that predicted.

For Cascade II operating at 60 kV, as predicted the jitter for the triggered gap is decreased, however there is little effect on the overall jitter associated with the switch which remains of the order of 90 ns.

When the voltage across Cascade II is increased to 70kV the jitter observed in switch operation drops to 12.8ns and there is good agreement between the predicted jitter for the individual gaps in the cascade and the observed behaviour of the switch.

VII. CONCLUSIONS & FUTURE WORK

The triggered behaviour of a corona controlled cascade has been investigated at atmospheric pressure in ambient air. Using a simple cascade, switching operation has been achieved with a jitter of less than 15ns.

Estimates for the expected jitter in switch operation have been made. These were based on data on the triggered breakdown of the individual gaps, combined with predictions of the expected voltages across the gaps in the cascade calculated from the corona emission behaviour established for the electrodes. The experimental data gathered on cascade operation appears to demonstrate the validity of the approach.

The operation of the cascade has been monitored using Rogowski and D-dot probes and information on the changes in current flowing into the cascade and the voltage across the cascade during triggered operation have been reported.

To further develop understanding of the behaviour of corona controlled cascades it will be necessary in future to:

determine the corona emission characteristics for the electrodes over a range of pressures in air;

determine the breakdown behaviour for single corona gaps over a wider range of both d.c. and triggering voltages and over a wider range of pressures;

investigate the relationships between the predicted behaviour of the time to breakdown and jitter for individual gaps in the cascade and the breakdown time and jitter of the cascade.

This approach should allow the design of cascade switches with well-defined and predictable characteristics

In addition it will be important to model the electrical behaviour of the switch as it operates to check the validity of the diagnostic measurements reported in this paper and to determine how the voltage across the cascade gaps is redistributed during switch operation. This may provide insights to allow the performance of the switch to be optimised.

VIII. REFERENCES

[1] J. M. Koutsoubis, and S.J. MacGregor, "Effect of gas type on high repetition rate performance of a triggered, corona stabilised switch", IEEE Trans. Dielectr. Electr. Insul., Vol. 10, pp. 245-255, 2003.

[2] S.J. MacGregor, S.M. Turnbull, F.A. Tuema, and O. Farish, "Factors affecting and methods of improving the pulse repetition frequency of pulse-charged and dc-charged high-pressure gas switches", IEEE Trans. Plasma Sci., Vol. 25, pp. 110-117, 1997.

[3] J. R. Beveridge, S. J. MacGregor, M. J. Given, I. V. Timoshkin and J. M. Lehr. "A Corona-stabilised Plasma Closing Switch", IEEE Trans. Dielectr. Electr. Insul., Vol. 16, pp 948–955, 2009

[4] M.J.Given, I.V. Timoshkin, M.P. Wilson, S.J. MacGregor. "A Novel Design for a Multistage Corona Stabilised Closing Switch. IEEE Trans. Dielectr. Electr. Insul., Vol. 18, pp 983–989, 2011

[5] R.S. Sigsmond "Simple approximate treatment of unipolar space charge dominated coronas: The Warburg law and the saturation current". J.Appl. Phys. Vol 53 pp 891-898, 1982